

Estimating Ground and Other Planes from a Single Tilted Laser Range Finder for On-Road Driving

Yasovardhan Reddy E, Hemanth Korrapati and K Madhava Krishna

Abstract—We present a method for extracting ground and other planes from a single non rotating laser mounted on a slow moving car used for on-road driving. A laser scan is decomposed into linear clusters. Corresponding clusters from subsequent scans are merged to form planes. The ground plane is identified based on the current vehicle height and the variance in height of the planes. Once these seed planes are identified future scan points either get associated with these planes or result in formation of new planes. Scan points that do not belong to any of the plane are left as such in the representation. Since the robustness of the method is contingent on how a single scan is decomposed into linear clusters, we compare the quality of the terrain representation due to three such clustering methods, one by iterative end point fit, other by adaptive breakpoint detection and thirdly the current method based on adaptive cosine similarity.

I. INTRODUCTION

On-road navigation is a crucial component of autonomous navigation outdoors and presents interesting challenges, the prominent among those being the ability to discern the traversability of a terrain patch. Unlike in planar worlds where anything that the range scanner detects is considered to be an obstacle, in 3D terrains such easy classification is not possible as perceived obstacles are not necessarily at right angles to the currently traversed plane.

Outdoor navigation is significant for automation of robots that act as sentries and guards in big university campuses and firms where the terrain includes roads along with trees and plantations. It is a key component for automating outdoor vehicles that are required to interpret the terrain for safe autonomous driving. In this paper we present an algorithm for representing the local terrain of the vehicle in terms of planes and points to discern the traversable region. The algorithm finds with respect to the current robot pose the areas that are navigable. The exploration process involves the use of a GPS and AHRS for obtaining the state of the vehicle with respect to a global reference frame. The transformation of the laser frame with the vehicle is known. The laser is tilted such that the readings hit the terrain below.

The algorithm has been tested on real-time laser data obtained from a Maruti-Omni Vehicle and a Pioneer P3DX robot at our university campus. The algorithm has been able to classify navigable and non-navigable regions and is able to identify the traversable roads for successful navigation.

This work is supported by grants from CVRDE, India
Yasovardhan and Hemanth are graduate students at the Robotics Research Center, IIT Hyderabad while K Madhava Krishna is a faculty at the same center
mkrishna@iiit.ac.in

Three parts constitute the algorithm. The first part consists of decomposing a scan line into linear clusters. The second part involves merging clusters obtained across a set of N initial scanlines to form planes. The ground plane and other planes are identified in the process through the popular RANSAC based approach. Clusters of points that are not amenable to plane parametrization are left as such in the representation. In the third part we associate clusters from the most recent, $N + 1$, scanline to planes formed so far. Clusters that get associated to planes within a threshold leads to re-parametrization of those planes based on most recent data. Clusters that do not get associated with any of the planes are maintained as such and could result in formation of new planes in the future. The algorithm is thus able to recognize from every new scanline the continuation of the ground plane. If such a continuation of a ground plane is halted as new scanline clusters do not get associated with the current ground plane, the algorithm then identifies among the newly formed planes that which is most easily navigable from the currently traversed ground plane. This identified plane becomes the incumbent ground plane.

We compare three methods of forming clusters from a scanline of points. One is the popular iterative end point fit [6], the second is due to an adaptive breakpoint detection [2] and third the method of this paper based on an adaptive cosine similarity measure. We show that the adaptive breakpoint detection algorithm, abbreviated as ABD henceforth is conservative in decomposition of clusters and hence tends to have points on the kerbs as part of the road cluster. This is because the parameter λ [2] denoting the worst case incident angle is rather difficult to determine for outdoor data.

The novelty of this effort includes the use of plane parametrization from scanline data obtained incrementally to discern the ground plane from other planes as well as to identify the subsequently navigable planes when ground plane continuation is halted. The subsequently navigable planes are determined based on the angles made by their normals with the current ground plane. The paper also presents a new adaptive cosine similarity rule for forming clusters from scanline data and evaluates it with other known methods in the context of outdoor data. Previous approaches that have compared scan line clustering algorithms from laser range finders have done so predominantly on indoor data only [1], [3].

The method of using RANSAC over clustered data such as in this approach has been found to determine plane parameters better than making use of RANSAC to determine the inliers from an entire point cloud data and associating

them with the ground plane. This not so surprising intuition has been verified among other places in a most recent paper on Connected Component -RANSAC or CCRANSAC [5]. It is also more apt for real-time situations due to its inherent divide and conquer like philosophy.

Efficient detection and parametrization of ground and other planes as well as classification of navigable regions as shown in the section on experimental results confirms the efficacy of the proposed method.

II. LITERATURE REVIEW

Literature related to current effort includes feature extraction from laser scan line data and outdoor representations for efficient navigation. There have been several approaches to extract features from line segment data and a comparison of various popular methods such as the iterative end point fit [6] based split and merge algorithm, RANSAC[7], regression models, Hough Transform [8] and EM based approaches has been presented in [3]. There it was reported that the iterative end point fit based split and merge algorithm to be the most reliable as far as decomposing scanline data into linear clusters. Similar results were obtained in [1] where a fuzzy based split and merge algorithm with adaptive line breaking was proposed. The algorithm was extended to detect curve like clusters in [2]. However the relative efficacy of these methods in relatively sparse data obtained in largely unstructured outdoor terrains have not been reported. Moreover determining the apt incidence angle λ [1], [2] has been difficult for outdoor terrain and the performance of these methods depend crucially on this parameter. The use of planes to represent indoor data has also been experimented with. In [11] an EM algorithm clusters a dense 3D into its component planes. However it may be quite difficult to use this approach for incremental scan line data in a real-time scenario since the EM iterates to find the best clusters.

Many outdoor terrain representation methods work towards extracting the dominant planar patch from a point cloud like data. For example [14] uses RANSAC to extract the dominant plane from stereo data. However the susceptibility of such an approach to adequately estimate the dominant plane in presence of multiple structures has been well reported [4]. In a very recent contribution the authors in [5] propose a CCRANSAC approach that overcomes the problems of evaluating the dominant or ground plane by using RANSAC only on a set of points that belong to the same connected component. The current method is akin to this approach since it applies RANSAC only on clustered data to parametrize the planes rather than invoking RANSAC itself to extract the dominant plane cluster. In [9] Wolf and Sukhatme present a method to segregate the ground plane from the surrounding grassy areas through a HMM based approach. An Extended Kalman Filter based algorithm for road kerb detection is presented in [12]. The method assumes an indefinite continuation of ground plane and does not attempt to classify the data into navigable and non-navigable regions. The assumption that the roads are always bordered by kerbs need not always be the case in various parts of the

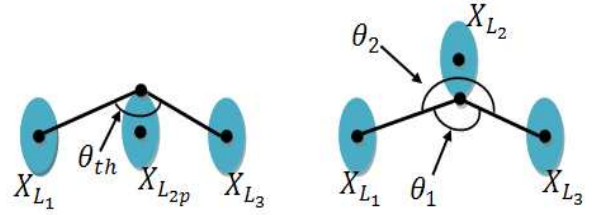


Fig. 1. (Left) Computing the threshold angle θ_{th} based on the uncertainty ellipses. (Right) The angle maximum(θ_1, θ_2) is compared with θ_{th} to decide the breakpoint.

world as well. In [13] a method for obstacle detection and avoidance in vegetated terrain is presented using a 3D Swiss Laser. There have also been approaches due to vision such as a fast color segmentation approach [10] for ground plane extraction that are not cited here for brevity of space.

III. THE METHOD

We first delineate the notations used before detailing the method.

A. Notations:

L, G, V : The coordinate frames of Laser, Ground and Vehicle frames.

S_L^t : Scan at time t ; a set of n measurements expressed in laser frame as $S_L^t = \{(P_{L_1}^t, \phi_{L_1}^t), (P_{L_2}^t, \phi_{L_2}^t), \dots, (P_{L_n}^t, \phi_{L_n}^t)\}$

$P_{L_i}^t$: Distance to a terrain point as measured by the i_{th} laser ray cast at $\phi_{L_i}^t$.

$\phi_{L_i}^t$: Angle of the i_{th} laser ray.

$X_{L_i}^t$: State of the i_{th} measurement of laser in its own frame
 $= [x_{L_i}^t, y_{L_i}^t]^T = [P_{L_i}^t \cos \phi_{L_i}^t, P_{L_i}^t \sin \phi_{L_i}^t]^T$

X_V^t : State of i_{th} measurement in V frame.

X_G^t : State of i_{th} measurement in G frame.

R_G : State of vehicle in G frame $= [R_{x_G}, R_{y_G}, R_{z_G}]$

$C^t = \{C_1^t, \dots, C_m^t\}$: A set of m linear clusters formed from the scan at time instant t , S^t

C_L^t, C_i^G, C_V^t : The cluster C at time t as represented in the laser, ground and vehicle frames.

Any member $C_{L_i}^t \in C_L^t$ is a set of some q points εS_L^t , i.e.
 $C_{L_i}^t = \{[x_{L_m}^t, y_{L_m}^t]^T, \dots, [x_{L_{m+q}}^t, y_{L_{m+q}}^t]^T\}$ Note that the points in a cluster are in angular sequence as obtained by the scan.

$d_{L_{ij}}^t$: Distance between two points $X_{L_i}^t, X_{L_j}^t$

$\theta_{L_{ijk}}^t$: Angle between the line joining $X_{L_i}^t, X_{L_j}^t$ and $X_{L_j}^t, X_{L_k}^t$

We have used the terms States and points synonymously.

B. Formation of Linear Clusters:

Consider three points, $X_{L_i}, X_{L_j}, X_{L_k}$, obtained in an angular sequence from the scan S_L^t . Then $\theta_{L_{ijk}}^t$ is found by the cosine similarity measure $\cos(\theta_{L_{ijk}}^t) = \frac{V_{L_{ij}} \cdot V_{L_{jk}}}{\|V_{L_{ij}}\| \|V_{L_{jk}}\|}$, where $\overline{V_{L_{ij}}}$ is the vector joining X_{L_i}, X_{L_j} .

If $\theta_{L_{ijk}}^t < \theta_{th}$ then then points are accumulated into the same cluster else X_{L_i} is discarded and the operation proceeds by considering the next set of 3 point $X_{L_j}, X_{L_k}, X_{L_l}$. θ_{th} is

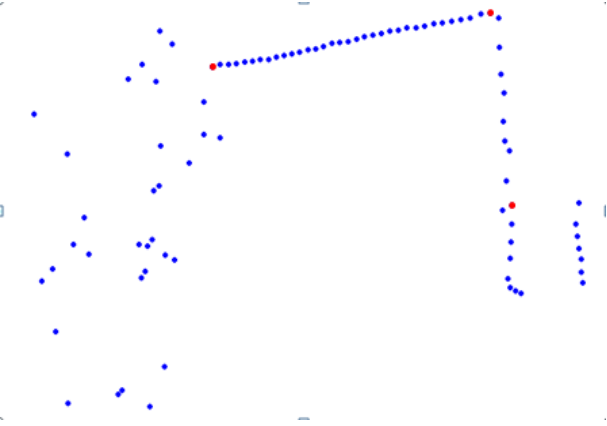


Fig. 2. A single laser scan with breakpoints shown in red.

adapted based on the distances $d_{L_{ij}}, d_{L_{jk}}$. If these distances are bigger θ_{th} is smaller and vice-versa.

Fig. 1 shows three such points $X_{L_1}, X_{L_2}, X_{L_3}$ and the uncertainty surrounding those point by ellipses. This uncertainty is essentially the uncertainty associated with the measurement

$[P_{L_i}, \phi_{L_i}]$ represented by the covariance matrix $\begin{bmatrix} \sigma_{L_i}^2 & 0 \\ 0 & \sigma_{L_i}^2 \end{bmatrix}$.

This uncertainty is transformed to the covariance matrix representing uncertainty in X_{L_i} , which results in the ellipses shown in Fig. 1. Then angle θ_{th} computed as follows. We project the center of the uncertainty ellipse of X_{L_2} onto the line joining X_{L_1} and X_{L_3} and denote it as X_{L_2p} as shown in Fig. 1. The angle formed by the line connecting the midpoint of X_{L_1}, X_{L_3} with the endpoint of the projected uncertainty ellipse of X_{L_2} defines the threshold angle θ_{th} . Then the maximum of the two angles made by the center of the ellipses of X_{L_1}, X_{L_3} with the endpoints of the original uncertainty ellipse of X_{L_2} (when it is not projected onto the line joining X_{L_1}, X_{L_3}) is found as shown in Fig. 1. If the maximum of these two angles is greater than θ_{th} , i.e. $\max(\theta_1, \theta_2) \geq \theta_{th}$ then the three points belong to the same cluster else a new cluster starts from X_{L_2} . Thus θ_{th} adapts with the distances $d_{L_{ij}}$ and hence claimed as the adaptive cosine similarity measure.

Points are then considered in the angular sequence three at a time and accumulated into a cluster if they satisfy the adaptive similarity. A new cluster is started whenever similarity is violated. When the cosine similarity is applied only by considering three consecutive points, there is a certain lack of memory that can result in a long cluster overlooking the breakpoints. To overcome this whenever more than ten consecutive points get accumulated in the same cluster, the cosine similarity is reformed by taking the endpoints of the current cluster along with an arbitrarily chosen point in between. This process is repeated a few times by choosing different points in the middle to detect breaks or change in slope in order to split the cluster is required.

Fig. 2 shows the formation of clusters for a scan line data of an outdoor terrain. The breakpoints where cosine similarity are violated also shown.

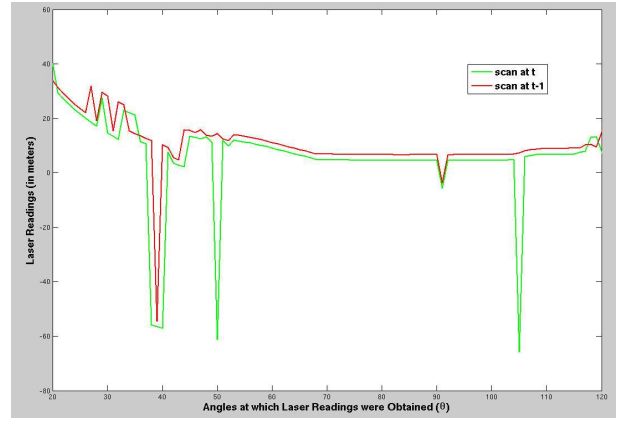


Fig. 3. The scan points belonging to the current cluster (in green) correlated with scan points of the previous cluster (in red).

C. Merging clusters to form seed planes:

For every cluster $C_{L_i}^t \in C_L^t$ we find the cluster $C_{L_j}^{t-1} \in C_L^{t-1}$ that has the maximum correlation with $C_{L_i}^t$. If the correlation measure between them is greater than a threshold the clusters are merged. The correlation is done as convolution like operation as shown in Fig. 3, where the smaller of the clusters is moved over the large one to find the set of points that offer the highest correlative measure.

Define correlation measure between $C_{L_i}^t$ and $C_{L_j}^{t-1}$ where $C_{L_i}^t$ has s points and $C_{L_j}^{t-1}$ has r points, $s > r$ as

$$C_{M_{ij}} = \max_k \left[\frac{1}{\sum_{i,j=1}^r (P_{L_{i+k}}^t - P_{L_j}^{t-1})^2} \right] \forall k \in [1, s-r]$$

Then for every cluster $C_{L_i}^t \in C_L^t$ the index j of the cluster $C_{L_j}^{t-1}$ from previous scan with which $C_{L_i}^t$ gets merged is found

$$\text{as } j = \underset{k}{\operatorname{argmax}} \left[C_{M_{ik}} \right].$$

Clusters that are merged in this manner for k such scans are plane parameterized to form the seed plane.

D. Ground plane Identification

Based on the current height of the laser obtained from the GPS and AHRS readings, we predict the distance measurements to the ground plane. We find to which of the formed seed planes these predicted distances correlate the best such that the correlation measure is greater than a threshold; that seed plane is identified as the ground plane.

E. Plane Continuation:

The seed planes formed from the initial k scans are extended in the subsequent scans by a resource allocation like process, merging the current scan clusters with the planes formed so far. Considering the set of clusters of current scan C_G^t to be the process and the set of planes P_L to be the resources, we find the best pair $(C_{G_i}^t, P_{L_j})$; $C_{G_i}^t \in C_G^t, P_{L_j} \in P_L$ which gives the smallest median perpendicular distance from the point in the cluster to the plane

$$(C_{G_i}^t, P_{L_j}) = \underset{i', j'}{\operatorname{argmin}} \left(M_d \operatorname{Pd} (C_{G_{i'}}^t, P_{L_{j'}}) \right)$$

$$i' = 1 \rightarrow m, j' = 1 \rightarrow p.$$

$M_d \operatorname{Pd} (C_{G_i}^t, P_{L_j})$ is the median perpendicular distance of the points in $C_{G_i}^t$ to the plane P_{L_j} .

If the median distance of the best match pair is less than a threshold the pair is removed from the allocation process, this allocation continues till all clusters are allocated or there exists no more planes or if the median distance threshold was exceeded. $C_{G_i}^t$ is a cluster of points in the G frame as mentioned before. The transformation between frames given by $X_{G_i} = T_V^G + R_V^G R_L^V X_{L_i}$, where T_V^G is the translation of the vehicle from the origin of the ground frame (usually the starting location of the vehicle) and R_A^B is the rotation of frame A with respect to B .

The unalloted clusters are retained in the terrain representation as such and after every k samples unallocated clusters are tested for merging conditions with existing planes or for the formation of a new seed plane.

F. Navigability Decision:

When ground plane continuation is halted the next navigable plane is identified as that plane whose normal with the normal of the currently halted ground plane has the least angular difference which can be negotiated by the vehicle.

Overall Algorithm

- 1) Starting Phase:
 - a) For first k time instants do
 - i) $C_L^k \leftarrow$ Obtain Linear Clusters (S_L^k)
 - ii) $C_{Mg}^k \leftarrow$ Merge clusters (S_L^k, C_{Mg}^{k-1});
 C_{Mg}^k is the list of merged clusters at instant k
 - b) SP \leftarrow Form Seed Planes (C_{Mg}^k)
 - c) GP \leftarrow Identify Ground plane ($SP, R_G, P_L^1, \dots, P_L^k$)
 - d) PL \leftarrow SP
 - e) If ($\operatorname{not}(\operatorname{IsIdentifiedGroundPlane}())$)
 - i) $\operatorname{EndOfNavigation} \leftarrow \operatorname{true}$
 - f) go to Phase 2
- 2) Subsequent Phase:
 - a) while ($\operatorname{not}(\operatorname{EndOfNavigation}())$) do
 - b) for next k instants do
 - i) PL \leftarrow MergeClusterToPlane(PL, C_G^k)
 - ii) $C_{NM}^k \leftarrow$ Merge Cluster (C_{NM}^k, C_{NM}^{k-1}); C_{NM}^k are clusters in C_L^k not merged to planes in PL.
 - iii) if $\operatorname{not}(\operatorname{GroundPlaneContinued})$ Fl \leftarrow False
 - c) SP \leftarrow Form seed Planes(C_{NM}^k)
 - d) if not (Fl)
 - if $\operatorname{not}(\operatorname{FoundNextNavigablePlane}(\operatorname{GP}, \operatorname{SP}))$
 $\operatorname{EndOfNavigation} \leftarrow \operatorname{True}$.
 - else
Append(PL, SP); Append seed planes in SP to the list of planes, PL

IV. EXPERIMENTAL RESULTS



Fig. 4. The experimental set up with the measuring devices mounted on the Maruti-Omnivision

Terrain modeling experiments were performed on a Maruti-Omnivision Vehicle that was mounted with a Sick Laser Range Finder (LRF), Sirf3 based GPS and an attitude head reference system (AHRS) from Xsens inc. The vehicle traveled at around 10kph. The experimental setup on the vehicle is shown in Fig 4. The terrain is represented using OSG Graphics Library.

The top left image of Fig. 5 in the next page depicts the front view of a part of the road as seen from the vehicle. Top right image of Fig. 5 shows the representation of the terrain as computed by our algorithm. The seed plane is shown in yellow and the subsequently navigable planes in green. The boundary between two navigable ground planes is shown in Magenta. The non navigable planes are shown in cyan, clusters that could not form planes are shown as red dots. Top middle image shows the point cloud representation of the scene. Similarly, in the bottom row ground and side plane formation of another scene is shown. Background of the scene is shown in Navy blue in the middle and right images.

We compare the performance of three clustering algorithms on the basis of how accurately they extract the ground plane. The algorithms evaluated are the iterative end-point fit (IEPF), the adaptive breakpoint detection (ABD) and adaptive cosine similarity (ACS). The ground truth data is more readily obtainable for the road regions of the terrain than the non ground regions such as bushes, kerbs, trees and people. Hence the comparison is done based on the accuracy of ground plane extraction than other parts of the terrain.

TABLE I
COMPARISON OF CLUSTERING OF SCAN POINTS METHODS

Map No.	ABD		IEPF		ACS	
	FP	FN	FP	FN	FP	FN
Map 1	30.305	3.809	0.586	0.795	0.418	4.73
Map 2	1.672	1.564	1.832	0.402	0.089	3.753
Map 3	12.247	56.6	0.324	38.687	0.324	17.842

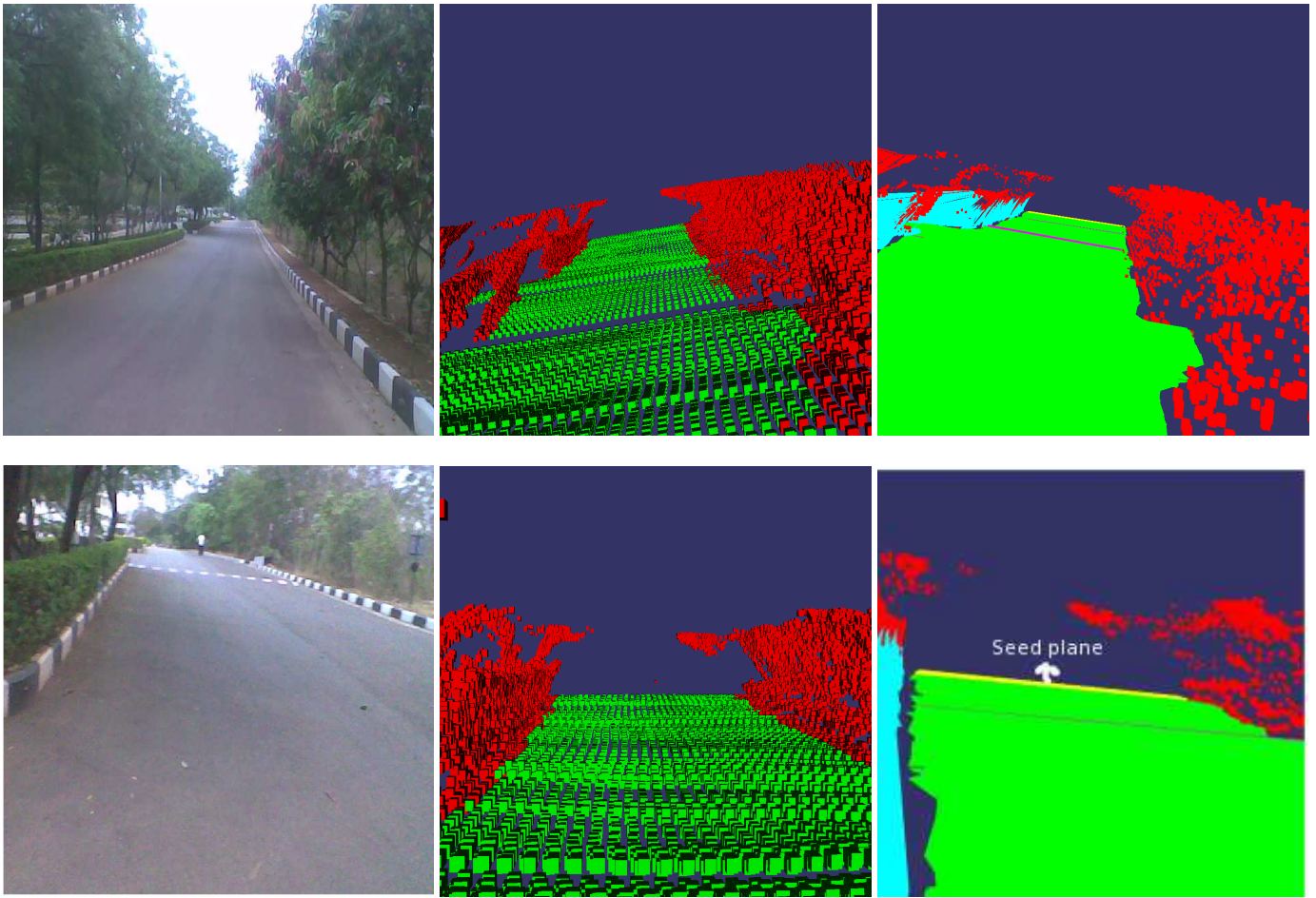


Fig. 5. In the top row, actual image is in top left, top middle image is point-cloud representation of the image (green is navigable and red non-navigable) and top right image is the representation of terrain in ground and other planes. Similarly, in the bottom row another scene is represented

Table I tabulates the comparisons. The first column corresponds to various maps on which the comparisons were performed. The second and third columns show the percentage of false positives and false negative classification of ground plane by the ABD method, the fourth and fifth for the IEPF method and the last two columns for the proposed ACS method. The false positive and false negative percentages are obtained for each scan line data once the ground plane is formed and then averaged over subsequent scans till the mapping terminates. The average values are reported in the table. The ground truth data is available as width of the road between the kerbs. For a given state of the robot it is possible to estimate then, those angular sequence of points that would hit the ground. The false positive and negatives can then be computed. The λ value used in the ABD was 10 since it gave the best clusters for various values of λ tried between 5 and 100. It can be seen from the tabulations that the performance of ACS and IEPF methods were generally better than ABD in terms of positive. This is because the ABD tends to miss out the kerbs, thereby increasing the length of ground plane cluster resulting in more false positives.

The method is applicable for outdoor navigation, for identifying the next best region to navigate based on the

angles between the various planes formed. Since we were more interested in classification rather than accurate mapping of the outdoor data, we have relied on a GPS with 1m resolution and linearly interpolated scans obtained between two GPS waypoints onto the terrain. This has not in any ways affected the classification process on numerous experiments we have performed thus far.

REFERENCES

- [1] G. A. Borges and M. Aldon, "Line extraction in 2D range images for mobile robotics", *Journal of Intelligent and Robotic Systems*, 40, pp. 267- 297, 2004
- [2] Pedro Nunez, et. al, "Feature Extraction from Laser Scan Data based on Curvature Estimation for Mobile Robotics", *ICRA*, pp 1167-1172, 2006
- [3] Viet Nguyen, Agostino Martinelli, Nicola Tomatis, Roland Siegwart, "A Comparison of Line Extraction Algorithms using 2D Laser Rangefinder for Indoor Mobile Robotics", *IROS*, 2005
- [4] C.V. Stewart, "Bias in robust estimation caused by discontinuities and multiple structures", *IEEE Transactions on Pattern Analysis and Machine Intelligence*, 19(8):818833,1997
- [5] Orazio Gallo, Roberto Manduchi, and Abbas Rafii, "Robust Curb and Ramp Detection for Safe Parking Using the Canesta TOF Camera", *Computer Vision and Pattern Recognition Workshops, CVPR Workshops 2008*
- [6] R.O. Duda and P.E. Hart, *Pattern Classification and Scene Analysis*, Wiley, NY.

- [7] M. A. Fischler and R. C. Bolles, "Random sample consensus: a paradigm for model fitting with applications to image analysis and automated cartography.", *Commun. ACM*, 24(6):381-395, 1981.
- [8] J. Illingworth and J. Kittler, "A survey of the Hough transform", *Comput. Vision Graph. Image Process.*, 44(1):87-116, 1988.
- [9] Denis F. Wolf and Gaurav S. Sukhatme, "Semantic Mapping Using Mobile Robots," 2007. *IEEE Transactions on Robotics*, 2007.
- [10] Morten Rufus Blas, Motilal Agrawal, Aravind Sundaresan, Kurt Konolige, "Fast Color/Texture Segmentation For Outdoor Robots" *IEEE-RSJ Intl. Conf on Robots and Systems*, 4078-4083, 2008.
- [11] R. Triebel, W. Burgard, and F. Dellaert, "Using Hierarchical EM to Extract Planes from 3D Range Scans", *IEEE Intl. Conf. on Robotics and Automation*, 2005.
- [12] W.S. Wijesoma, K.R.S. Kodagoda and A Balasuriya, "Road-Boundary Detection and Tracking Using Ladar Sensing", *IEEE-TRA*, 20(3), 2004
- [13] H Schafer, A Hach, et. al, "3D Obstacle Detection and Avoidance in Vegetated Off-Road Terrain", *IEEE-RSJ Intl. Conf on Robots and Systems*, 2008
- [14] Motilal Agrawal, Kurt Konolige and Robert C. Bolles, "Localization and Mapping for Autonomous Navigation in Outdoor Terrains : A Stereo Vision Approach", *WACV*, 2007